

Published in final edited form as:

Biochim Biophys Acta. 2009 August ; 1791(8): 730–739. doi:10.1016/j.bbali.2009.03.012.

Downregulation of Neutral Ceramidase by Gemcitabine: Implications for Cell Cycle Regulation

Bill X. Wu^a, Youssef H. Zeidan^a, and Yusuf A. Hannun^{a,*}

^a Department of Biochemistry and Molecular Biology, Medical University of South Carolina, Charleston, SC 29425, USA

SUMMARY

Gemcitabine (GMZ) is a chemotherapeutic agent with well established effects on cell growth arrest and apoptosis. In this study, we investigated the potential roles of bioactive sphingolipids in mediating the growth suppressing effects of GMZ on a polyoma middle T transformed murine endothelial cell line. After 12-hour GMZ (0.6 μ M) treatment, cell growth was arrested at the G₀/G₁ phase as detected by flow cytometric cell cycle analysis and MTT cell viability analysis, and this was accompanied by dephosphorylation of the retinoblastoma protein (Rb). Furthermore, GMZ treatment resulted in increased levels of specifically the very long chain ceramides as determined by mass spectrometry. Mechanistically, GMZ did not appear to affect the activities of many enzymes of ceramide metabolism; however, GMZ caused a selective reduction in the protein levels of neutral ceramidase (NCDase), as indicated by Western blot analysis, with a concomitant decrease in NCDase activity. The significance of NCDase loss on cell cycle regulation was investigated by specific knockdown of the enzyme using small interfering RNA (siRNA). Interestingly, NCDase siRNA transfection was sufficient to induce a cell cycle arrest at G₀/G₁ and an increase in total ceramide levels, with significant elevation in very long chain ceramides (C_{24:1} and C_{24:0}). NCDase siRNA also induced Rb dephosphorylation. These data provide evidence for a novel mechanism of action for GMZ and highlight downregulation of NCDase as a critical step in GMZ-mediated ceramide elevation and cell cycle arrest.

Keywords

Neutral ceramidase; Ceramide; Cell cycle arrest; Gemcitabine; Sphingolipid

INTRODUCTION

Sphingolipids, first identified as important structural components of cell membranes, are currently recognized as critical regulators and mediators of various biological responses [1, 2]. Among these bioactive species, ceramide, sphingosine (SPH), ceramide-1-phosphate, and sphingosine-1-phosphate (S1P) have been extensively studied and identified as essential bioactive molecules in mediating cellular signaling pathways, including cell growth arrest, differentiation, apoptosis, chemotaxis, and inflammation [3–6].

*Corresponding author: Dr. Yusuf A. Hannun, Department of Biochemistry and Molecular Biology, Medical University of South Carolina, 173 Ashley Ave., Charleston, SC 29425, USA. Tel: +1 843 792 9318; f ax: +1 843 792 4322, hannun@musc.edu.

Publisher's Disclaimer: This is a PDF file of an unedited manuscript that has been accepted for publication. As a service to our customers we are providing this early version of the manuscript. The manuscript will undergo copyediting, typesetting, and review of the resulting proof before it is published in its final citable form. Please note that during the production process errors may be discovered which could affect the content, and all legal disclaimers that apply to the journal pertain.

Several lines of evidence indicate that ceramide is involved in mediating/regulating cell cycle arrest. Rani et al. showed that inhibition of glucosylceramide synthase resulted in accumulation of endogenous ceramide and resulted in an arrest of the cell cycle in NIH 3T3 cells [7]. Treatment with exogenous C6-ceramide induced a dose-dependent arrest in the G0/G1 phase of the cell cycle in human diploid fibroblast and Molt-4 cells [8]. Exogenous C6-ceramide also blocked the progression of the cell cycle at the G0/G1 phase in ovarian granulosa cells [9]. Moreover, it has been shown that both endogenous ceramide generated by bacterial sphingomyelinase (SMase) and exogenous ceramide could induce a significant drop in telomerase activity, as well as cell cycle arrest in G0/G1 without detectable cell death in human lung carcinoma cell line [10,11]. Another study showed that up-regulation of a neutral SMase, nSMase2, caused G0/G1 cell cycle arrest and an increase in ceramide, especially in the very long chain C(24:1) and C(24:0) ceramides. Conversely, down-regulation of nSMase2 by siRNA reversed the effects of cell cycle arrest and resulted in decreased levels of very long chain ceramides [12,13]. Further, a recent study showed that knock down of either isoform of sphingomyelin synthase, SMS1 or SMS2, by siRNA resulted in an increase of ceramide levels, decrease of sphingomyelin levels and cell growth arrest [14]. However, the role of endogenous enzymes of ceramide metabolism in regulating ceramide-dependent cell cycle progression has not been well defined.

In the course of studying the potential role of ceramide in mediating the cytotoxic and growth suppressing action of GMZ, a critical chemotherapeutic agent, we found that GMZ selectively regulates the levels of very long chain ceramides, and that GMZ selectively regulated the activity of NCDase.

Among various enzymes that regulate the turnover and levels of ceramides, ceramidases (CDases) catalyze the hydrolysis of ceramide to form SPH and free fatty acid. Thus, ceramidases could play important roles in the regulation of the substrate ceramide, the immediate product SPH, and the further downstream metabolite S1P. According to the catalytic pH optima and primary sequence, CDases have been classified into alkaline CDases, acid CDase, and NCDase. Phylogenetic analysis reveals that the three CDase families are derived from different ancestral genes [15]. Among the CDases, several alkaline CDases have been cloned and characterized, including phytoCDase (YPC1p) and dihydroCDase (YDC1p) from yeast *Saccharomyces cerevisiae* [16,17], a homologue of YPC1p (haPHC) from human [18] and a mouse alkaline ceramidase (maCER1) [19]. A single acid CDase enzyme has been characterized and its mutations cause the human disorder Farber's disease [20].

Several reports have suggested that NCDase is regulated in response to cytokines and growth factors, and that this enzyme may have important roles in the regulation of ceramide in response to these stimuli and in mediating some of its actions on apoptosis and/or cell growth regulations. It has been reported that platelet-derived growth factor up-regulates NCDase activity in rat mesangial cells [21], and the enzyme activity was modulated in a bimodal manner by interleukin-1 β in rat hepatocytes [22], leading to a decrease in ceramide concomitant with an increase in SPH. Similarly, it was shown that NCDase activity increased and ceramide levels decreased following IL-1 β stimulation of rat mesangial cells [23] whereas nitric oxide led to degradation of NCDase [23,24]. In mesangial cells, NCDase could also mediate the effect of advanced glycation end-products (generated during chronic hyperglycaemia) on cell proliferation [25]. In *Drosophila*, mutation of NCDase causes synaptic dysfunction with impaired vesicle fusion and trafficking [26]. Moreover, targeted expression of NCDase rescued *Drosophila* mutants from retinal degeneration [27]. However, the role of NCDase in cell growth regulation has not been well studied.

In this study, we investigated the effects of GMZ on ceramide levels and metabolism in middle-T transformed murine endothelial cells (H. end. FB). We provide evidence that NCDase is an

important regulator of cell cycle arrest, linking the biological consequences of knocking down the enzyme to its biochemical role as a regulator of sphingolipid metabolism.

MATERIALS AND METHODS

Reagents

All biochemicals were from Sigma (St. Louis, MI) unless otherwise stated. [choline-methyl-¹⁴C] Sphingomyelin was provided by the Lipidomics Core Facility at the Medical University of South Carolina. All other lipids were purchased from Avanti Polar Lipids (Alabaster, AL). Culture media were obtained from Invitrogen.

Cell Cultures

The H. end. FB murine endothelial cell line was a generous gift from Dr. F. Bussolino (University of Turin, Turin, Italy). Cells were grown in 100-mm dishes in Dulbecco's Modified Eagle Medium (DMEM) supplemented with 10% fetal bovine serum and maintained at 37 °C in a humidified atmosphere of 5% CO₂. Cells were plated at a density of 0.3–0.4 × 10⁶ cells in a 100-mm plate the day before the experiments. GMZ was dissolved in water to 100 mM, diluted in PBS, and added directly to the cultured cells for treatment.

MTT and Trypan Blue Exclusion Assays

5 × 10⁴ H. end. cells were plated in 6-well plates overnight and then were treated with 0.6 μM GMZ for various periods (0–18 hours), MTT solution was added to the cells and incubated at 37 °C for two more hours. Then, MTT solubilization solution (10% Triton X-100 in acidic isopropyl alcohol, 0.1 N HCl) was added to the cells overnight. Colorimetric measurements were obtained in a microplate reader (Molecular Devices) at 595 nm, and background was subtracted at 650 nm.

For determination of cell viability, control and GMZ treated cells were counted using a hemocytometer in the presence of trypan blue solution at a 1:1 ratio (v/v) (Sigma), as described by the manufacturer.

Analysis of Cell Cycle Profiles by Flow Cytometry

After treatment of H. end. cells with 0.6 μM GMZ for 12 hours or NCDase RNAi for 36 hours, the cells were treated with trypsin and centrifuged. The cell pellet was washed twice with ice-cold PBS and then fixed in 70% ethanol at 4 °C. On the day of analysis, cells were washed with PBS and treated with 20 μg/ml RNase A at 37 °C for 30 min. Cells were then stained with 100 μg/ml propidium iodide for 30 min and analyzed with a FACStarPLUS flow cytometer (BD Biosciences).

Western Blot analysis

The cells were collected in lysis buffer (50 mM Tris, pH 7.5, 0.2% Triton-X100) and homogenized by brief sonication. The homogenate was centrifuged for 10 min at 800 × g at 4 °C, and the supernatant was used for protein determination using BCA Assay (Bio-Rad Laboratories, CA). Thirty μg of total proteins from each lysate were loaded onto 4–20% gradient SDS polyacrylamide gels, subjected to electrophoresis, and then transferred to polyvinylidene difluoride membranes. The blots were probed using 1:1000 dilution of primary antibodies followed by horseradish peroxidase labeled secondary antibody (1:2000 dilution) (Santa Cruz Biotechnology, Inc., CA). The signals were detected using ECL chemiluminescence reagents (Pierce, IL). The antibodies against phospho-S795 Rb, PARP, and Caspase-3 were from Cell Signaling Technology, Inc. (Boston, MA). The monoclonal antibody against total Rb was from BD Pharmingen (Franklin Lakes, NJ). The β-actin antibody

was purchased from Sigma (St. Louis, MI) The antibody against mouse NCDase was a generous gift from Dr. Richard Proia at the National Institute of Diabetes and Digestive and Kidney Diseases.

Real Time RT-PCR

Total RNA from cells was isolated using the Qiagen minikit for total RNA extraction. Complementary DNA was synthesized from 1 µg of total RNA using SSII reverse transcriptase (Invitrogen) and an oligo(dT) primer. Real time RT-PCR was performed on an iCycler system (Bio-Rad, Hercules, CA) using SYBR Green PCR reagents (Bio-Rad, Hercules, CA). The first steps of RT-PCR were 2 min at 50 °C followed by a 10-min hold at 95 °C. Cycles (n = 40) consisted of a 15 s melt at 95 °C, followed by a 60 s at 60 °C. The final step was 60 s incubation at 60 °C. Reactions were performed in triplicate. The PCR primers used in this study were as follows: β -actin (forward, 5'-ATTGGCAACGAGCGGTTCC-3'; reverse, 5'-TGTAGTTTCATGGATGCCACA-3') and NCDase (forward, 5'-ACCACACACCCTGTCTGCATAC-3'; reverse, 5'-TCGGGACCACTGCTCATGTTG-3'). The β -actin gene was used as an internal reference control to normalize relative levels of gene expression. Real time PCR results were analyzed using Q-Gene® software [28], which expresses data as mean normalized expression. Mean normalized expression is directly proportional to the amount of RNA of the target gene relative to the amount of RNA of the reference gene.

Assays of Neutral and Acid SMase Activities

In vitro SMase enzymatic assays were performed as described previously with modifications [12,29]. Briefly, H. end. cells were collected and lysed as described above. For assays of acid SMase, fifty µg of protein were adjusted to a total volume of 100 µl of reaction mixture, which contains 1 mM of EDTA, 250 mM sodium acetate (pH 5.0), 100 mM (choline-methyl-¹⁴C) sphingomyelin and 0.1% Triton X-100. After incubation for 1 hour at 37 °C, the reaction was stopped by adding 1.5 ml of chloroform/methanol (2:1), followed by adding 200 µl of water. Phases were separated by centrifugation at 2000 × g for 5 min. By subjecting 400 µl of the upper phase to scintillation counting, acid SMase activity was determined by quantification of the amount of released radioactive phosphocholine.

For neutral SMase activity, the reaction mixture contained 100 mM Tris (pH 7.4), 10 mM MgCl₂, 0.2% Triton X-100, 10 mM dithiothreitol, and 100 µM [choline-methyl-¹⁴C] sphingomyelin (10 cpm/pmol) and phosphatidylserine (6.7 mol %). The procedures and quantification of neutral SMase activity was the same as that for acid SMase activity described above.

CDase Enzymatic Assays

Detection of CDase enzymatic activity was performed according to previously described methods [25,30] with slight modifications. Briefly, H. end cell lysates were prepared as described above, and 50 µg lysate was subjected to reactions of acid, neutral or alkaline CDase activities. Acid CDase activity was measured using detergent/lipid mixed micelles with D-erythro-C₁₂-NBD-ceramide, a characterized substrate for CDase activity assays [31], at a concentration of 50 µM or 1.08 mol% in a 250 mM sodium acetate (pH 5.0) (contained 1 mM CaCl₂, 0.3% (w/v) Triton X-100 final concentration, with a total volume of 100 µl. For the assays of neutral or alkaline CDase activities, acetate buffer was replaced by 200 mM Tris buffers (pH 7.0 for neutral and 9.0 for alkaline ceramidase activities, respectively). The reaction mixtures was incubated at 37 °C for 1 hour. Conversion of NBD-C12 ceramide to NBD-dodecanoic acid were detected by spotting the organic phase on a TLC plate. Results were quantitated by densitometric analysis using ImageQuant software.

RNA Interference Transfection

Synthetic sense and antisense oligonucleotides were purchased from Qiagen (Lafayette, CO). A DNA sequence (aatgacagtcacacagtggc) was selected for the mouse NCDase and a nonspecific siRNA was used as control. Transfection of siRNAs into H. end. cells was performed by Nucleofector (Amaxa, Cologne, Germany) using Cell Line Nucleofector Kit T. H. end. cells were harvested and resuspended in Nucleofector solution at 1.5×10^6 cells/100 μ l. After addition of 120 pmol siRNA oligonucleotides, the cells were transfected by Nucleofector program T-24. Then, the cells were plated into 10 cm or 6-well plates. The transfected cells were applied to various analysis 24–48 hours after the transfection.

LC/MS Analysis of Endogenous Ceramides

Sphingolipid analysis was performed in the Lipidomics Core Facility of the Medical University of South Carolina, using Electrospray Ionization/Tandem Mass Spectrometry (ESI-MS/MS) on a Thermo Finnigan TSQ 7000 triple stage quadrupole mass spectrometer and operating in a multiple reaction monitoring positive ionization mode [32].

Measurement of Caspase-3 Activity

Caspase-3 activity was determined using the caspase-3 colorimetric assay (R&D Systems) according to the manufacturer's instructions. Briefly, H. end. cells transfected with SCR or NCDase RNAi were lysed in the supplied lysis buffer. The supernatants were collected and incubated with the supplied reaction buffer at 37 °C. The levels of caspase-3 enzymatic activity are directly proportional to the fluorescence signal detected using a fluorescent microplate reader. Caspase-3 activity levels were normalized to total protein amounts for each sample.

Statistical Analysis

Results are expressed as the mean \pm SD. Comparisons among groups were made by Student's *t* tests. A *P* value of 0.05 or less was considered as statistically significant.

RESULTS

Effects of GMZ on H. end Cell Cycle

GMZ, an important chemotherapeutic agent, can induce either cell growth arrest or apoptosis in cultured cells. To evaluate the effects of GMZ on H. end. cells, MTT and cell cycle analysis were employed. First, the cells were exposed to 0.6 μ M GMZ for various periods (0–18 hours) and then subjected to MTT assays. As shown in Fig. 1A, GMZ-induced inhibitory effects on cell growth started at 12 hours after treatment, and became more prominent after 18 hours. However, as measured by trypan blue exclusion assay, there was no significant change in cell viability following GMZ treatment up to 24 hours (Fig. 1B). Next, the effects of GMZ on cell growth arrest and apoptosis were further examined using flow cytometry. As shown in Fig. 1C, the cell cycle profile of control cells resembled that of normal exponentially growing cells, with 36.2 \pm 9.7 % of the cells in G0/G1 and 51.8 \pm 11.1 % in S phase. In contrast, after 12 hours GMZ treatment, cells were retained in the G0/G1 phase, with 59.7 \pm 4.7 % of cells in G0/G1 and 35.7 \pm 4.0 % in S phase. Of note, there was no detectable apoptosis in GMZ treated cells, consistent with the results of the trypan blue exclusion assay. The data reveal that GMZ induces preferentially an arrest in the G0/G1 phase of the cell cycle.

To explore the mechanisms involved in the cell cycle (G1) arrest caused by GMZ treatment, the phosphorylation status of Rb was examined next. Rb is critical for cell cycle progression as it regulates the G1/S phase restriction point. Rb protein can be phosphorylated at multiple sites. While hyperphosphorylated forms of Rb (pRb) are primarily found in proliferating cells, the hypophosphorylated forms of Rb are found mainly in resting cells and are mechanistically

linked to cell cycle arrest in G0/G1. Western blotting was performed using antibodies specifically recognizing total Rb or the S795 phosphoserine of Rb.

As shown in Fig. 1D, whereas the hyperphosphorylated forms of Rb predominated in control cells, Rb became dephosphorylated as shown by the lower bands after 12-hour GMZ treatment. To further confirm the dephosphorylation of Rb, we examined the phosphorylation of S795, which has been shown to regulate the association of Rb with E2F1, a transcription factor critically involved in the G1/S-phase transition of the mammalian cell cycle [33]. Consistently, a 75% decrease of phosphorylation of serine S795 in Rb was detected. Together, these data demonstrate that GMZ treatment, at relatively low concentrations, results in cell growth arrest instead of apoptotic effects. Also, the GMZ induced effects of cell cycle inhibition are linked to Rb activation (dephosphorylation).

Induction of Ceramide by GMZ Treatment

Our previous studies showed that increases of ceramide, especially very long chain ceramide, are important for cell cycle arrest induced by cell confluence [13]. Also, ceramide plays a role in the regulation of Rb activation. Thus, it became of interest to examine if GMZ induced significant changes in ceramide and then determine if these changes play a role in the response to GMZ treatment. H. end. cells were collected at 3, 6, 12, and 18 hours after exposure to GMZ, and sphingolipids were extracted and analyzed by LC/MS. As shown in Fig. 2A, total ceramide increased by 35% at 12 hours following GMZ treatment. Among the major ceramide species (C16, C24:1, C24 ceramides), significant elevation was observed predominantly in the very long chain ceramide, 24-ceramide (1.8-fold) and less so in C24:1- ceramide (1.4-fold) at 12 hour (Fig. 2B). These results show specific changes in ceramide species following GMZ administration.

Downregulation of NCDase by GMZ Treatment in H. end. Cells

The above results suggested that GMZ might affect specific pathways/enzymes of ceramide metabolism. To begin to identify which sphingolipid enzymes may be responsible for the ceramide accumulation induced by GMZ treatment, the enzymatic activities of SMases and CDases were examined (Fig. 3). GMZ treatment did not appear to modulate the enzymatic activities of acid and alkaline ceramidases (Fig. 3A and 3B) or acid and neutral SMases (Fig. 3D and 3E). On the other hand, a significant time dependent decrease was observed in the activity of NCDase (Fig 3C). Significant downregulation (~50%) of NCDase activity was observed at 12 hours. The effect of GMZ on NCDase protein levels was confirmed by Western blot analysis using an antibody specifically-developed against mouse NCDase. Major bands were detected between about 95 kDa to 135 kDa. The multiple band pattern may due to due to complexity of modifications, such as O-glycosylation [34] and N-glycosylation [35]. The antibody specificity was also confirmed using lysates of hepatocytes from NCDase KO mice by western blot analysis (supplemental figure 1). The results showed that GMZ induced significant loss of NCDase, especially at the 12 and 24-hour time points (Fig. 4A). Further, to evaluate if the loss of NCDase was caused by inhibition of transcription, the mRNA level of NCDase was analyzed by real time RT-PCR; however, no significant changes were observed in the mRNA levels of NCDase during GMZ treatment (Fig. 4B). The down-regulation effect of GMZ on NCDase protein level was also dose-dependent. After 12-hour exposure to GMZ, while a low concentration (0.1 μ M) GMZ showed no significant effect on NCDase level, higher concentrations of GMZ treatment caused a dose-dependent downregulation of both NCDase activity (Fig. 4C) and protein levels (Fig. 4D). 2 μ M GMZ led to a nearly complete loss of NCDase protein. As GMZ caused cell cycle arrest, it was of interest to examine if other growth arresting stresses can also down-regulate NCDase level. As shown in Fig 4E, 12-hour serum starvation also induced down-regulation of NCDase protein and enzymatic activity, further proving that NCDase protein is cell cycle regulated.

Down-regulation of NCDase Using siRNA

To determine the role of downregulation of NCDase in GMZ responses and cell growth regulation, siRNA was developed to knockdown NCDase. The effectiveness and specificity of NCDase siRNA were first established by transfecting H. end. cells with NCDase siRNA or with control siRNA (SCR) that exhibits no homology to any mouse DNA sequence based on a BLAST search. As shown in Fig. 5A and 5B, siRNA to NCDase resulted in a specific loss both at mRNA and protein levels. Next, NCDase activity was examined and as shown in Fig. 5B, NBD-dodecanoic acid was measured on a TLC plate to quantify the product of NCDase activity. NCDase activity in NCDase siRNA transfected cells was much lower (~80%) than the SCR control cells (Fig. 5C and 5D). This decrease of NCDase activity correlated with the decrease in protein levels. Moreover, those changes were in the same range seen with GMZ.

Modulation of Ceramide Levels by Knockdown NCDase Using siRNA in H. end. Cells

Based on the above results, it became of interest to determine the ceramide molecular species that are modulated by NCDase siRNA. Using electrospray/MS/MS analysis, the changes in ceramide species were analyzed in SCR control and NCDase knockdown cells. The level of total ceramide increased by 38% in NCDase knockdown cells compared with control (Fig 6A). Importantly, NCDase knockdown resulted in specific elevation of the very long chain ceramides C24:1 and C24:0 which increased significantly by 66 % and 112 %, respectively, as compared with control cells (Fig. 6B). Interestingly, NCDase RNAi did not result in decreased levels of either SPH or S1P. As SPH can be regulated by other enzymes, including at least 4 other ceramidases, knockdown of neutral ceramidase alone may not cause significant changes to sphingosine levels. Moreover, S1P effect on GMZ response were examined. As shown in Supplemental figure 2, no significant difference was observed on GMZ effects by comparing BSA vehicle and S1P treatment using MTT assays. Thus, it is unlikely that S1P play major role in the GMZ effects. Taken together, these results demonstrate a role for NCDase in regulating very long chain ceramides, which may be important for control of cell growth.

Effects of Down-regulation of Endogenous NCDase on Cell Cycle

To determine whether the GMZ-induced down-regulation of NCDase plays a role in regulating growth, we examined whether loss of NCDase affects cell growth. H. end. cell proliferation was evaluated using MTT assay, and cells were analyzed on days 1, 2, and 3 after the down-regulation of NCDase by siRNA. As shown in Fig. 7A, cells transfected with NCDase siRNA results in a cell growth pattern similar to the serum starved cells, and much slower than SCR siRNA treated cell. Noteworthy, cell growth started to recover in the third day after NCDase siRNA treatment. This recovery might be caused by the increased portion of untransfected cells which were proliferating normally through the three days. These results demonstrate that down-regulating endogenous NCDase inhibits H. end. cell growth.

To further determine how NCDase modulates cell growth, the cell cycle was analyzed by flow cytometry in cells transfected by the NCDase siRNA. As shown in Fig. 7B, 36 hours after NCDase siRNA transfection, $57.7\pm 6.2\%$ of the cells became arrested in the G0/G1 phase and $33.3\pm 0.3\%$ were in the S phase of the cell cycle. In contrast, in cells treated with the nonspecific siRNA, $32.4\pm 1.3\%$ of the population was in the G0/G1 phase and $53.8\pm 0.2\%$ in the S phase of the cell cycle. These profiles are similar to normally growing untreated cells, demonstrating lack of effect of the nonspecific siRNA. Thus, down-regulation of NCDase resulted in an arrest of the cell cycle in G0/G1, mimicking the results previously seen with GMZ.

The flow cytometry analysis also showed that only $2.58\pm 1.7\%$ of the cells were apoptotic in the SCR control cells, possibly caused by the electroporation procedure (Nucleofector, Amaxa) during siRNA delivery. Interestingly, there was a slight increase ($5.7\pm 0.7\%$) of apoptotic cells after NCDase knockdown, suggesting minor apoptotic effects may also be caused by NCDase

siRNA. Further evaluate the effects of NCDase siRNA on apoptotic effects using PARP degradation by Western blotting and caspase 3 activity analyses confirmed that NCDase siRNA only induced minor cell death in H. end. cells (data not show), but resulted in more profound arrest in the cell cycle.

Downstream Targets for Downregulation of NCDase

Because pRb is an important regulator of the G1/S boundary in the cell cycle, and the above results showed that GMZ treatment induced the hypophosphorylation (activation) of Rb (Fig 8), we next attempted to determine the effect of NCDase siRNA on the state of Rb phosphorylation. The results in Fig. 8 show that whereas the majority of Rb protein was in a hyperphosphorylated form in the control SCR siRNA cells, while Rb was significantly dephosphorylated upon 24–48 hours NCDase siRNA treatment. Moreover, NCDase siRNA-induced hypophosphorylation of Rb was also detected by the S795 phosphoserine antibody. These effects on Rb activity provide specific links between the down-regulation of NCDase and cell cycle arrest.

DISCUSSION

In this study, we examined the role of ceramide in mediating actions of GMZ in H. end. cells and the mechanisms regulating ceramide accumulation, with specific focus on NCDase. GMZ caused NCDase down-regulation, resulting in ceramide accumulation. Mechanistically, specific knockdown of NCDase using RNAi was sufficient to increase ceramide levels, Rb dephosphorylation, and cell cycle arrest at G0/G1 in the H. end. cells. This study suggests that NCDase down-regulation is an essential step for mediating cell responses to GMZ in H. end. cells, and implicates endogenous NCDase as an important regulator of cell cycle arrest.

First, this study demonstrates that the NCDase/ceramide pathway participates in the response of H. end. cells to the action of GMZ, and specifically in the induction of cell cycle arrest. Indeed, ceramide metabolism has been linked to the regulation of cell cycle and chemotherapy-induced cell growth arrest or apoptosis [2]. Chemotherapeutic agents, such as cisplatin, daunorubicin, and vincristine can elevate endogenous ceramide levels in several cancer cells [36,37]. Moreover, ceramide accumulation has been observed with GMZ treatment [38]. However, the mechanisms, the specific ceramide species, and sphingolipid enzymes involved in this process were unclear. In this study, GMZ induced preferentially an arrest in the G0/G1 phase of the cell cycle rather than apoptosis in the H. end. cells. Further, the current results showed that GMZ induced a specific loss of NCDase protein, in a dose and time-dependent manner. The functional consequences of the loss of endogenous NCDase in response to GMZ were determined using siRNA to knockdown NCDase. These results showed that NCDase is required for clearance of ceramide as the levels of ceramide increased in the knock down. More importantly, the results showed that loss of NCDase resulted in a specific cell cycle arrest with dephosphorylation of Rb and a G0/G1 cell cycle arrest. The dephosphorylation of Rb, which might be mediated by the ceramide activated protein phosphatases [39], provides specific links between the decrease of NCDase and cell cycle arrest. Thus, these results suggest that the loss of NCDase in response to GMZ is sufficient to mediate cell cycle arrest, which is the main response of these cells to the stress action of GMZ.

In the NCDase knockdown cells, a specific elevation of the very long chain ceramides (C_{24:1} and C_{24:0}) was observed. These results extend previous in vitro studies that showed that NCDase preferentially cleaves very long chain ceramides as substrates [40]. Thus, NCDase manifests specific metabolic functions in cells. Moreover, our previous studies showed that elevation of ceramide levels, especially very long chain ceramides, are important to cell cycle arrest [13]. Thus, a picture is emerging whereby accumulation of very long chain ceramides

(either through induction of neutral sphingomyelinase or loss of NCDase) influences cell cycle arrest at the G0/G1 phase of the cell cycle.

The mechanism for GMZ induced degradation of NCDase is largely unknown. As no significant changes were observed in the mRNA levels of NCDase during GMZ treatment, the down-regulation of NCDase is likely to be caused by protein destruction. It is possible that the proteasome plays a role in this process. It has been shown previously that nitric oxide induced proteolytic loss of NCDase [24]. In addition, other DNA damage reagents have been shown to induce degradation of SPH kinase 1 by cathepsin enzyme [41]. It will be important to further determine if proteasome or lysosome play roles in the GMZ-induced NCDase degradation.

Unexpectedly, among various enzymatic activities of CDases and neutral/acid SMase, only NCDase activity was significantly modulated by GMZ treatment. In our experiments, the major ceramide species contributing to the total ceramides accumulations are very long chain ceramides, which are the favorite substrate of NCDase but not acid CDase [42]. Further, no significant change in ASMase activity was detected while a slight increase was observed for nSMase activity. These results illuminate the specific roles of NCDase in the GMZ pathway and cell regulation. Noteworthy, the activation of SMases could not be excluded as SMases might be also activated by modification of protein and/or translocation within cells [13,43]. Thus, the roles of various sphingolipid enzymes in the GMZ response still need to be further clarified.

The ability of NCDase to regulate cell growth leads to the suggestion that NCDase could contribute to tumor promotion and thus provides a novel potential target for cancer therapy. Supporting evidence derives from the observations that several ceramidase inhibitors are under investigation for cancer therapy. For example, D-MAPP, the inhibitor of NCDase, has been found to sensitize the radioresistance of squamous carcinoma cells by modulation of endogenous ceramide levels [44]. B13, a D-MAPP analog and non-lysosomal targeted ceramidase inhibitor, can reduce the viability of colon cancer by 90% [45]. B13 can also inhibit cell proliferation and/or induce apoptosis in several cancer cell lines, including, melanoma cells, an immortalized keratinocyte line [46] and prostate cancer cells [47]. A subsequent study screened RNA interference effects of a variety of genes and identified that the knockdown of the ceramide transport protein, CERT, can sensitize cancer cells to multiple chemotherapeutic agents, suggesting that RNA interference against sphingolipid related proteins could be an essential target for chemotherapy-resistant cancers [48]. As NCDase siRNA also results in cell growth arrest, it will be important to test if specific knockdown of NCDase *in vivo* can contribute to chemotherapy action.

Noteworthy, much higher (38 fold) NCDase activity and expression levels were detected in the polyoma middle T oncogene transformed endothelioma cells than in several other cells [49]. Middle T is a membrane protein that complexes with a number of proteins used by tyrosine kinase associated receptors to stimulate mitogenesis, and can be considered as a permanently active analogue of a receptor. As a result, the injection of the H.end cells into C57/BL wildtype or nude mice can lead to vascular tumors growth and death of the hosts [50]. Middle T oncoprotein can also be found to induce several other tumors, such as, breast cancer and bone tumors [51,52]. Thus, it will be interesting to further investigate whether the abnormally high NCDase level may play a role in the middle T oncogene response in the future.

In conclusion, this study provides significant insight into the metabolic and physiologic functions of NCDase by demonstrating that specific knockdown of NCDase resulted in accumulation of very long chain ceramides and in subsequent cell growth arrest. Thus, these results implicate for the first time endogenous NCDase as an important regulator of the cell cycle. More importantly, these data provide evidence for a novel mechanism of action for GMZ

and highlight downregulation of NCDase as a critical step in GMZ-mediated ceramide elevation and cell cycle arrest, suggesting that inhibition of NCDase may be a novel target for future cancer therapies.

Supplementary Material

Refer to Web version on PubMed Central for supplementary material.

Acknowledgments

This study was supported by NIH grant CA87584 and GM43825. We would like to thank the Lipidomics Core at the Medical University of South Carolina for expert assistance.

Abbreviations

CDase	ceramidase
NCDase	neutral ceramidase
SPH	sphingosine
S1P	sphingosine-1-phosphate
GMZ	gemcitabine
Rb	retinoblastoma protein
pRb	hyperphosphorylated forms of retinoblastoma protein
SMase	sphingomyelinase
siRNA	small interfering RNA
SCR	scrambled small interfering RNA

References

1. Hannun YA, Obeid LM. The Ceramide-centric universe of lipid-mediated cell regulation: stress encounters of the lipid kind. *The Journal of biological chemistry* 2002;277:25847–25850. [PubMed: 12011103]
2. Ogretmen B, Hannun YA. Biologically active sphingolipids in cancer pathogenesis and treatment. *Nat Rev Cancer* 2004;4:604–616. [PubMed: 15286740]
3. Taha TA, Hannun YA, Obeid LM. Sphingosine kinase: biochemical and cellular regulation and role in disease. *J Biochem Mol Biol* 2006;39:113–131. [PubMed: 16584625]
4. El Alwani M, Wu BX, Obeid LM, Hannun YA. Bioactive sphingolipids in the modulation of the inflammatory response. *Pharmacol Ther* 2006;112:171–183. [PubMed: 16759708]
5. Pettus BJ, Chalfant CE, Hannun YA. Ceramide in apoptosis: an overview and current perspectives. *Biochim Biophys Acta* 2002;1585:114–125. [PubMed: 12531544]
6. Modrak DE, Gold DV, Goldenberg DM. Sphingolipid targets in cancer therapy. *Mol Cancer Ther* 2006;5:200–208. [PubMed: 16505092]
7. Rani CS, Abe A, Chang Y, Rosenzweig N, Saltiel AR, Radin NS, Shayman JA. Cell cycle arrest induced by an inhibitor of glucosylceramide synthase. Correlation with cyclin-dependent kinases. *The Journal of biological chemistry* 1995;270:2859–2867. [PubMed: 7852361]
8. Jayadev S, Liu B, Bielawska AE, Lee JY, Nazaire F, Pushkareva M, Obeid LM, Hannun YA. Role for ceramide in cell cycle arrest. *The Journal of biological chemistry* 1995;270:2047–2052. [PubMed: 7836432]

9. Kim JH, Han JS, Yoon YD. Biochemical and morphological identification of ceramide-induced cell cycle arrest and apoptosis in cultured granulosa cells. *Tissue Cell* 1999;31:531–539. [PubMed: 10669928]
10. Ogretmen B, Schady D, Usta J, Wood R, Kravcka JM, Luberto C, Birbes H, Hannun YA, Obeid LM. Role of ceramide in mediating the inhibition of telomerase activity in A549 human lung adenocarcinoma cells. *The Journal of biological chemistry* 2001;276:24901–24910. [PubMed: 11335714]
11. Ogretmen B, Pettus BJ, Rossi MJ, Wood R, Usta J, Szulc Z, Bielawska A, Obeid LM, Hannun YA. Biochemical mechanisms of the generation of endogenous long chain ceramide in response to exogenous short chain ceramide in the A549 human lung adenocarcinoma cell line. Role for endogenous ceramide in mediating the action of exogenous ceramide. *The Journal of biological chemistry* 2002;277:12960–12969. [PubMed: 11815611]
12. Marchesini N, Luberto C, Hannun YA. Biochemical properties of mammalian neutral sphingomyelinase 2 and its role in sphingolipid metabolism. *The Journal of biological chemistry* 2003;278:13775–13783. [PubMed: 12566438]
13. Marchesini N, Osta W, Bielawski J, Luberto C, Obeid LM, Hannun YA. Role for mammalian neutral sphingomyelinase 2 in confluence-induced growth arrest of MCF7 cells. *The Journal of biological chemistry* 2004;279:25101–25111. [PubMed: 15051724]
14. Tafesse FG, Huitema K, Hermansson M, van der Poel S, van den Dikkenberg J, Uphoff A, Somerharju P, Holthuis JC. Both sphingomyelin synthases SMS1 and SMS2 are required for sphingomyelin homeostasis and growth in human HeLa cells. *The Journal of biological chemistry* 2007;282:17537–17547. [PubMed: 17449912]
15. Tani M, Okino N, Mori K, Tanigawa T, Izu H, Ito M. Molecular cloning of the full-length cDNA encoding mouse neutral ceramidase. A novel but highly conserved gene family of neutral/alkaline ceramidases. *The Journal of biological chemistry* 2000;275:11229–11234. [PubMed: 10753931]
16. Mao C, Xu R, Bielawska A, Obeid LM. Cloning of an alkaline ceramidase from *Saccharomyces cerevisiae*. An enzyme with reverse (CoA-independent) ceramide synthase activity. *The Journal of biological chemistry* 2000;275:6876–6884. [PubMed: 10702247]
17. Mao C, Xu R, Bielawska A, Szulc ZM, Obeid LM. Cloning and characterization of a *Saccharomyces cerevisiae* alkaline ceramidase with specificity for dihydroceramide. *The Journal of biological chemistry* 2000;275:31369–31378. [PubMed: 10900202]
18. Mao C, Xu R, Szulc ZM, Bielawska A, Galadari SH, Obeid LM. Cloning and characterization of a novel human alkaline ceramidase. A mammalian enzyme that hydrolyzes phytoceramide. *The Journal of biological chemistry* 2001;276:26577–26588. [PubMed: 11356846]
19. Mao C, Xu R, Szulc ZM, Bielawski J, Becker KP, Bielawska A, Galadari SH, Hu W, Obeid LM. Cloning and characterization of a mouse endoplasmic reticulum alkaline ceramidase: an enzyme that preferentially regulates metabolism of very long chain ceramides. *The Journal of biological chemistry* 2003;278:31184–31191. [PubMed: 12783875]
20. Sugita M, Dulaney JT, Moser HW. Ceramidase deficiency in Farber's disease (lipogranulomatosis). *Science* 1972;178:1100–1102. [PubMed: 4678225]
21. Coroneos E, Martinez M, McKenna S, Kester M. Differential regulation of sphingomyelinase and ceramidase activities by growth factors and cytokines. Implications for cellular proliferation and differentiation. *The Journal of biological chemistry* 1995;270:23305–23309. [PubMed: 7559485]
22. Nikolova-Karakashian M, Morgan ET, Alexander C, Liotta DC, Merrill AH Jr. Bimodal regulation of ceramidase by interleukin-1beta. Implications for the regulation of cytochrome p450 2C11. *The Journal of biological chemistry* 1997;272:18718–18724. [PubMed: 9228043]
23. Franzen R, Pautz A, Brautigam L, Geisslinger G, Pfeilschifter J, Huwiler A. Interleukin-1beta induces chronic activation and de novo synthesis of neutral ceramidase in renal mesangial cells. *The Journal of biological chemistry* 2001;276:35382–35389. [PubMed: 11457826]
24. Franzen R, Fabbro D, Aschrafi A, Pfeilschifter J, Huwiler A. Nitric oxide induces degradation of the neutral ceramidase in rat renal mesangial cells and is counterregulated by protein kinase C. *The Journal of biological chemistry* 2002;277:46184–46190. [PubMed: 12359735]

25. Geoffroy K, Wiernsperger N, Lagarde M, El Bawab S. Bimodal effect of advanced glycation end products on mesangial cell proliferation is mediated by neutral ceramidase regulation and endogenous sphingolipids. *The Journal of biological chemistry* 2004;279:34343–34352. [PubMed: 15184394]
26. Rohrbough J, Rushton E, Palanker L, Woodruff E, Matthies HJ, Acharya U, Acharya JK, Broadie K. Ceramidase regulates synaptic vesicle exocytosis and trafficking. *J Neurosci* 2004;24:7789–7803. [PubMed: 15356190]
27. Acharya U, Patel S, Koundakjian E, Nagashima K, Han X, Acharya JK. Modulating sphingolipid biosynthetic pathway rescues photoreceptor degeneration. *Science* 2003;299:1740–1743. [PubMed: 12637747]
28. Muller PY, Janovjak H, Miserez AR, Dobbie Z. Processing of gene expression data generated by quantitative real-time RT-PCR. *Biotechniques* 2002;32:1372–1374. 1376, 1378–1379. [PubMed: 12074169]
29. Zeidan YH, Pettus BJ, Elojeimy S, Taha T, Obeid LM, Kawamori T, Norris JS, Hannun YA. Acid ceramidase but not acid sphingomyelinase is required for tumor necrosis factor- α -induced PGE₂ production. *The Journal of biological chemistry* 2006;281:24695–24703. [PubMed: 16803890]
30. Wu BX, Snook CF, Tani M, Bullesbach EE, Hannun YA. Large-scale purification and characterization of recombinant *Pseudomonas* ceramidase: regulation by calcium. *J Lipid Res* 2007;48:600–608. [PubMed: 17164222]
31. Tani M, Okino N, Mitsutake S, Ito M. Specific and sensitive assay for alkaline and neutral ceramidases involving C12-NBD-ceramide. *J Biochem (Tokyo)* 1999;125:746–749. [PubMed: 10101288]
32. Bielawski J, Szulc ZM, Hannun YA, Bielawska A. Simultaneous quantitative analysis of bioactive sphingolipids by high-performance liquid chromatography-tandem mass spectrometry. *Methods* 2006;39:82–91. [PubMed: 16828308]
33. Wang J, Zhao Y, Kauss MA, Spindel S, Lian H. Akt regulates vitamin D₃-induced leukemia cell functional differentiation via Raf/MEK/ERK MAPK signaling. *Eur J Cell Biol* 2009;88:103–115. [PubMed: 19058874]
34. Tani M, Iida H, Ito M. O-glycosylation of mucin-like domain retains the neutral ceramidase on the plasma membranes as a type II integral membrane protein. *The Journal of biological chemistry* 2003;278:10523–10530. [PubMed: 12499379]
35. Mitsutake S, Tani M, Okino N, Mori K, Ichinose S, Omori A, Iida H, Nakamura T, Ito M. Purification, characterization, molecular cloning, and subcellular distribution of neutral ceramidase of rat kidney. *The Journal of biological chemistry* 2001;276:26249–26259. [PubMed: 11328816]
36. Bose R, Verheij M, Haimovitz-Friedman A, Scotto K, Fuks Z, Kolesnick R. Ceramide synthase mediates daunorubicin-induced apoptosis: an alternative mechanism for generating death signals. *Cell* 1995;82:405–414. [PubMed: 7634330]
37. Zeidan YH, Jenkins RW, Hannun YA. Remodeling of cellular cytoskeleton by the acid sphingomyelinase/ceramide pathway. *J Cell Biol* 2008;181:335–350. [PubMed: 18426979]
38. Chalfant CE, Rathman K, Pinkerman RL, Wood RE, Obeid LM, Ogretmen B, Hannun YA. De novo ceramide regulates the alternative splicing of caspase 9 and Bcl-x in A549 lung adenocarcinoma cells. Dependence on protein phosphatase-1. *The Journal of biological chemistry* 2002;277:12587–12595. [PubMed: 11801602]
39. Wolff RA, Dobrowsky RT, Bielawska A, Obeid LM, Hannun YA. Role of ceramide-activated protein phosphatase in ceramide-mediated signal transduction. *The Journal of biological chemistry* 1994;269:19605–19609. [PubMed: 8034729]
40. El Bawab S, Usta J, Roddy P, Szulc ZM, Bielawska A, Hannun YA. Substrate specificity of rat brain ceramidase. *J Lipid Res* 2002;43:141–148. [PubMed: 11792733]
41. Taha TA, El-Alwani M, Hannun YA, Obeid LM. Sphingosine kinase-1 is cleaved by cathepsin B in vitro: identification of the initial cleavage sites for the protease. *FEBS Lett* 2006;580:6047–6054. [PubMed: 17064696]
42. Momoi T, Ben-Yoseph Y, Nadler HL. Substrate-specificities of acid and alkaline ceramidases in fibroblasts from patients with Farber disease and controls. *Biochem J* 1982;205:419–425. [PubMed: 6814427]

43. Zeidan YH, Hannun YA. Activation of acid sphingomyelinase by protein kinase C δ -mediated phosphorylation. *The Journal of biological chemistry* 2007;282:11549–11561. [PubMed: 17303575]
44. Alphonse G, Bionda C, Aloy MT, Ardail D, Rousson R, Rodriguez-Lafrasse C. Overcoming resistance to gamma-rays in squamous carcinoma cells by poly-drug elevation of ceramide levels. *Oncogene* 2004;23:2703–2715. [PubMed: 15048093]
45. Selzner M, Bielawska A, Morse MA, Rudiger HA, Sindram D, Hannun YA, Clavien PA. Induction of apoptotic cell death and prevention of tumor growth by ceramide analogues in metastatic human colon cancer. *Cancer research* 2001;61:1233–1240. [PubMed: 11221856]
46. Raisova M, Goltz G, Bektas M, Bielawska A, Riebeling C, Hossini AM, Eberle J, Hannun YA, Orfanos CE, Geilen CC. Bcl-2 overexpression prevents apoptosis induced by ceramidase inhibitors in malignant melanoma and HaCaT keratinocytes. *FEBS Lett* 2002;516:47–52. [PubMed: 11959101]
47. Samsel L, Zaidel G, Drumgoole HM, Jelovac D, Drachenberg C, Rhee JG, Brodie AM, Bielawska A, Smyth MJ. The ceramide analog, B13, induces apoptosis in prostate cancer cell lines and inhibits tumor growth in prostate cancer xenografts. *Prostate* 2004;58:382–393. [PubMed: 14968439]
48. Swanton C, Marani M, Pardo O, Warne PH, Kelly G, Sahai E, Elustondo F, Chang J, Temple J, Ahmed AA, Brenton JD, Downward J, Nicke B. Regulators of mitotic arrest and ceramide metabolism are determinants of sensitivity to paclitaxel and other chemotherapeutic drugs. *Cancer Cell* 2007;11:498–512. [PubMed: 17560332]
49. Romiti E, Meacci E, Tani M, Nuti F, Farnararo M, Ito M, Bruni P. Neutral/alkaline and acid ceramidase activities are actively released by murine endothelial cells. *Biochem Biophys Res Commun* 2000;275:746–751. [PubMed: 10973793]
50. Garlanda C, Parravicini C, Sironi M, De Rossi M, Wainstok de Calmanovici R, Carozzi F, Bussolino F, Colotta F, Mantovani A, Vecchi A. Progressive growth in immunodeficient mice and host cell recruitment by mouse endothelial cells transformed by polyoma middle-sized T antigen: implications for the pathogenesis of opportunistic vascular tumors. *Proceedings of the National Academy of Sciences of the United States of America* 1994;91:7291–7295. [PubMed: 8041783]
51. Wang R, Bautch VL. The polyomavirus early region gene in transgenic mice causes vascular and bone tumors. *Journal of virology* 1991;65:5174–5183. [PubMed: 1654437]
52. Lin EY, Jones JG, Li P, Zhu L, Whitney KD, Muller WJ, Pollard JW. Progression to malignancy in the polyoma middle T oncoprotein mouse breast cancer model provides a reliable model for human diseases. *Am J Pathol* 2003;163:2113–2126. [PubMed: 14578209]

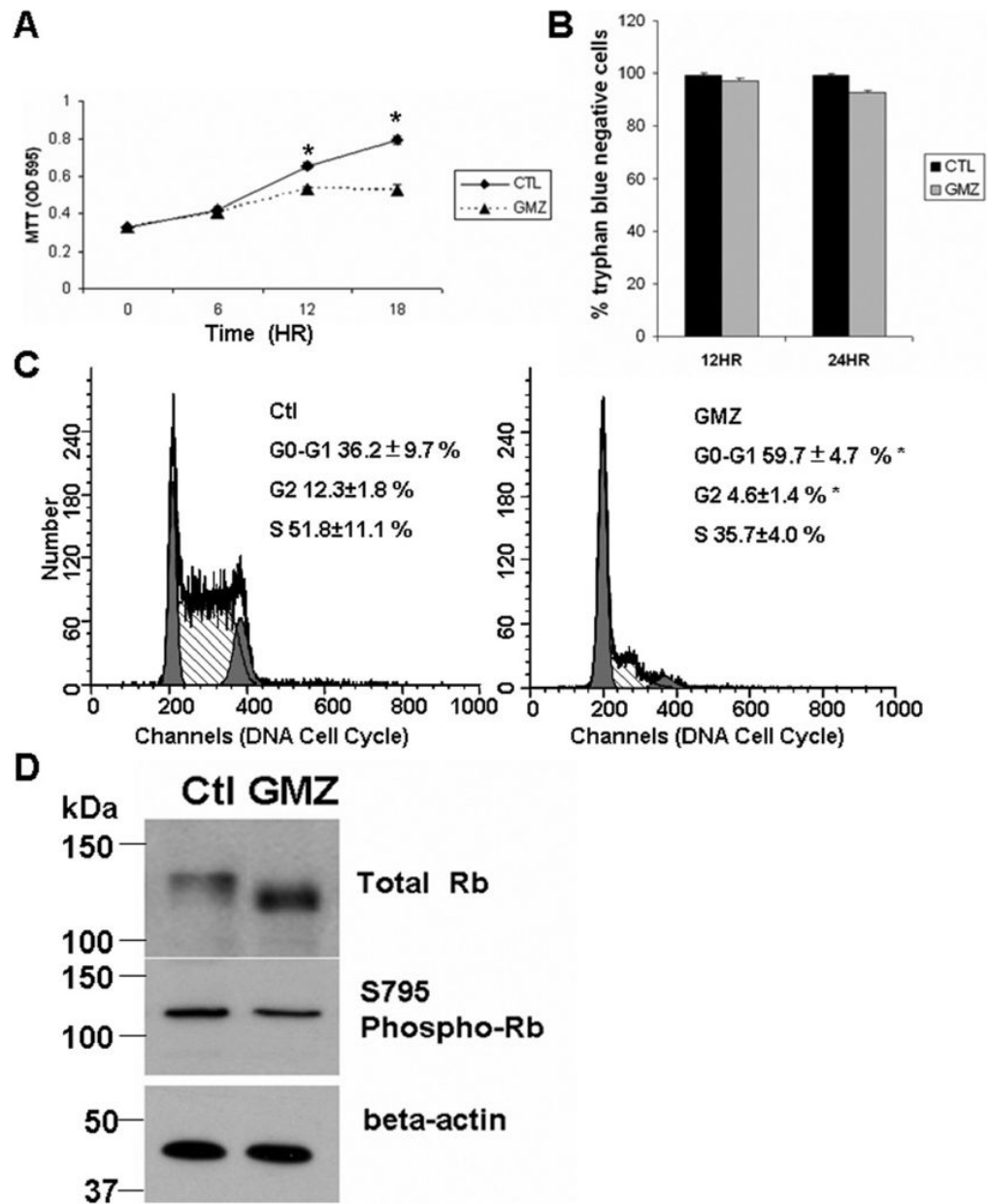


Figure 1. GMZ effects on cell growth, the cell cycle and pRb in H. end. FB cells

H. end. cells were cultured and treated with 0.6 μ M GMZ as described under “Material and Methods”. (A) The effects of GMZ on cell growth were determined by the MTT assay. (B) Cell viability was evaluated by trypan blue viability assays. (C) Cell cycle distribution profiles of control cells and cells treated with 0.6 μ M GMZ for 12 hours. (D) Effects of GMZ treatment on the state of Rb phosphorylation in H. end. cells using Western blot analysis. The results are representative of at least three independent experiments. For (A) and (B), the values are expressed as the mean \pm SD (n=3). CTL, control. *Significant differences in comparison of GMZ treatment to control ($P < 0.05$).

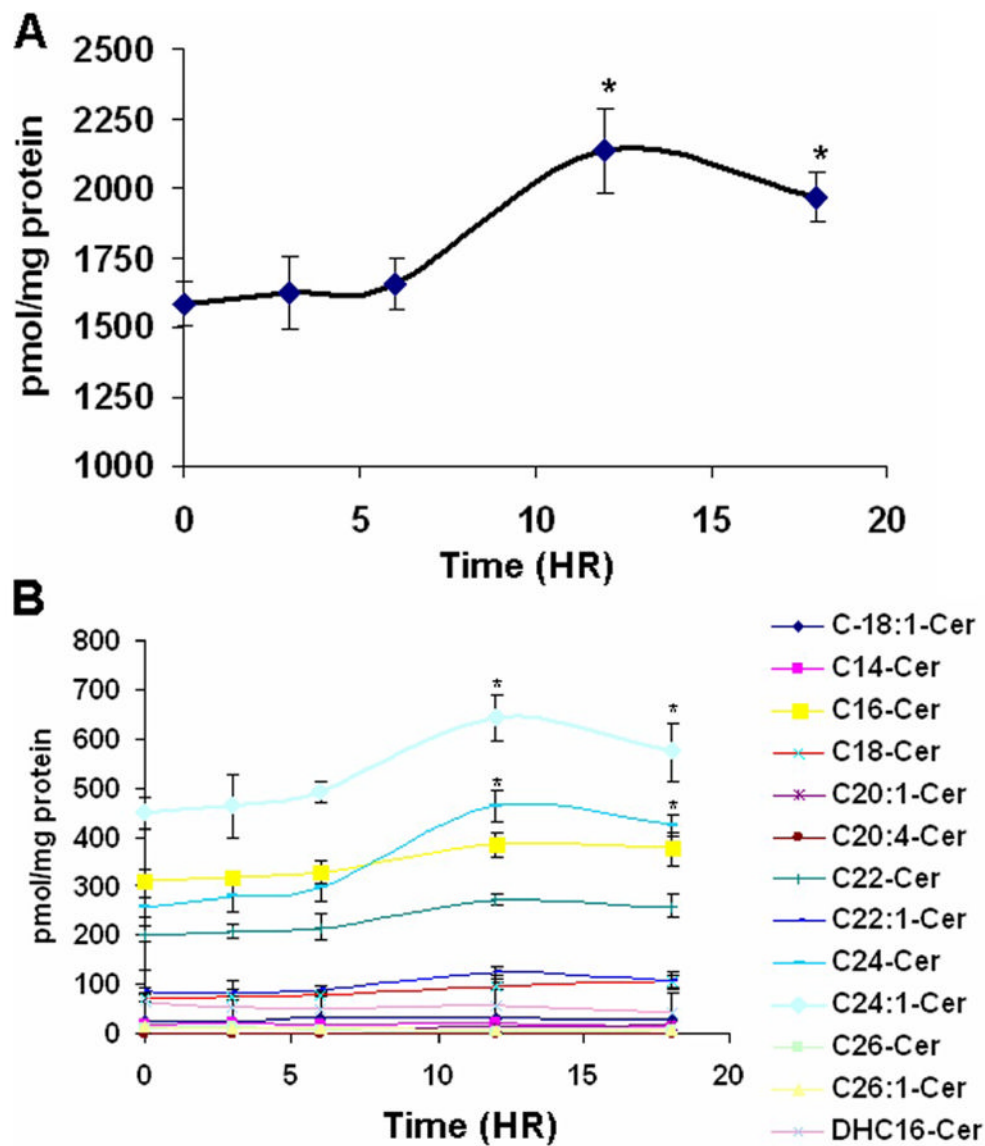
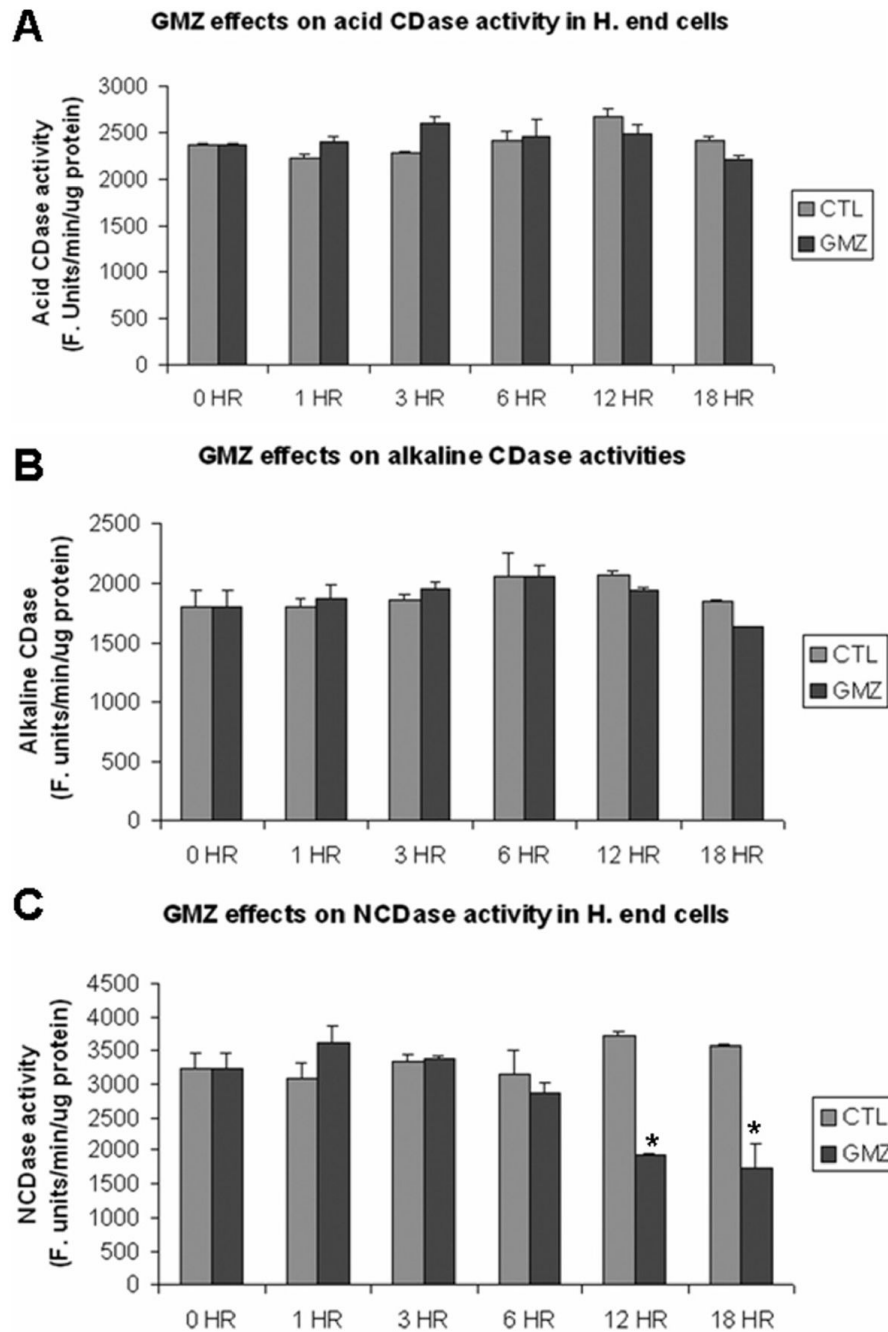


Figure 2. Modulation of ceramide species by GMZ

H. end. cells were seeded in 100 mm dishes and treated with 0.6 μ M GMZ. Cells were collected at 3, 6, 12, and 18 hours after treatment, and sphingolipids were extracted. Ceramide species were analyzed by mass spectroscopy and each sample was normalized to its respective total protein levels. (A) Total ceramide. (B) Ceramide species. The values are expressed as the mean \pm SD (n=3). The results are representative of two independent experiments. *Significant differences in comparison GMZ treatment to control ($P<0.05$).



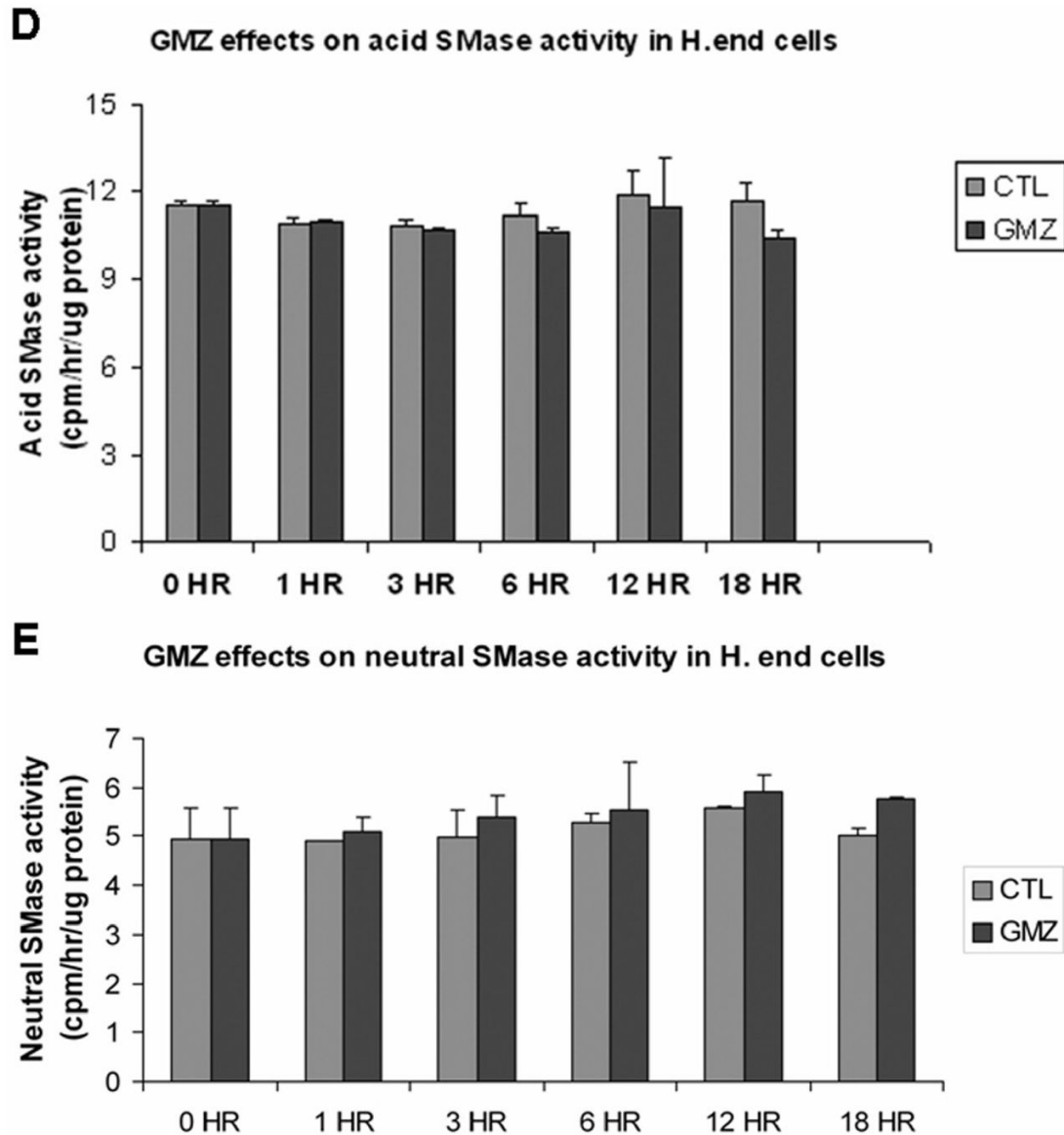


Figure 3. GMZ effects on sphingomyelinase and ceramidase activities

H. end. cells were treated with 0.6 μ M GMZ for various time points (0, 1, 3, 6, 12 and 18 hours). The cells were lysed and subjected to assays of SMase and ceramidase activities. (A) acid CDase activities. (B) Alkaline CDase activities. (C) NCDase activities. (D) Acid SMase activities. (E) Neutral SMase activities. The values are expressed as the mean \pm SD (n=3). The results are representative of at least two independent experiments. *Significant differences in comparison GMZ treatment to control ($P<0.05$).

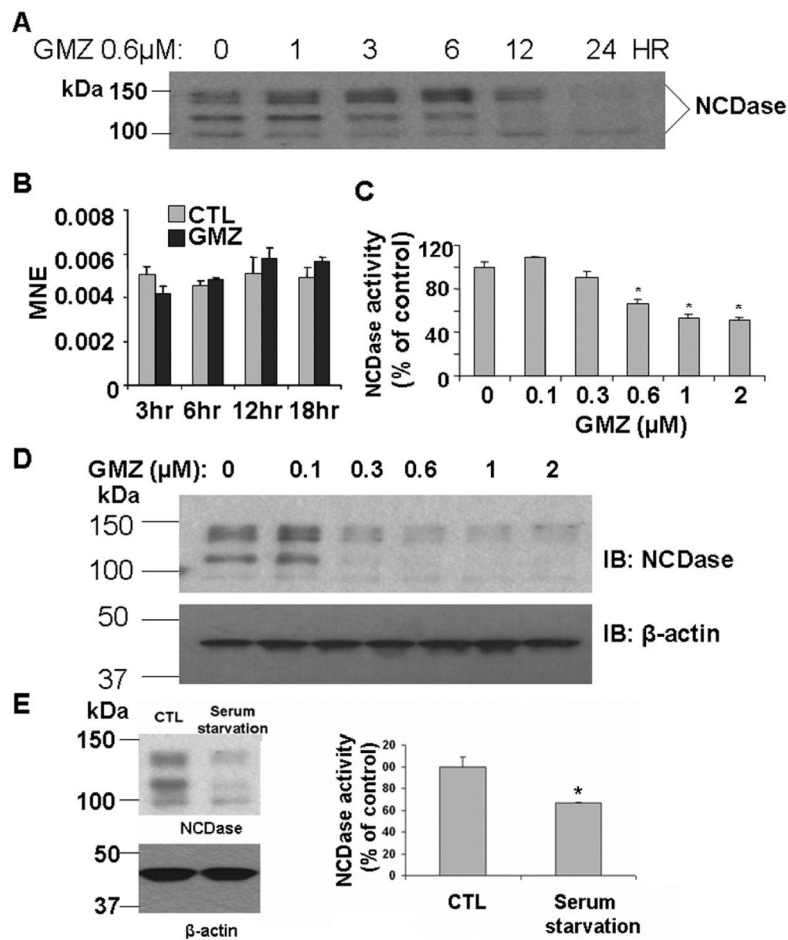


Figure 4. Down-regulation of NCDase by GMZ

Cells were treated with 0.6 μ M GMZ from 0–18 hours, and the levels of NCDase (A) protein and (B) mRNA were examined by Western blot and Real time RT-PCR as described under “Materials and Methods”. The dose effects (0–2 μ M) of GMZ on (C) protein and (D) activity levels of NCDase were evaluated after 12-hour exposure of GMZ. (e) Serum starvation effects on NCDase activity and protein. The values are expressed as the mean \pm SD (n=3). The results are representative of at least two independent experiments. IB, immunoblot; CTL, control; MNE, mean normalized expression. Statistical significance was calculated with respect to control (*, $p < 0.05$).

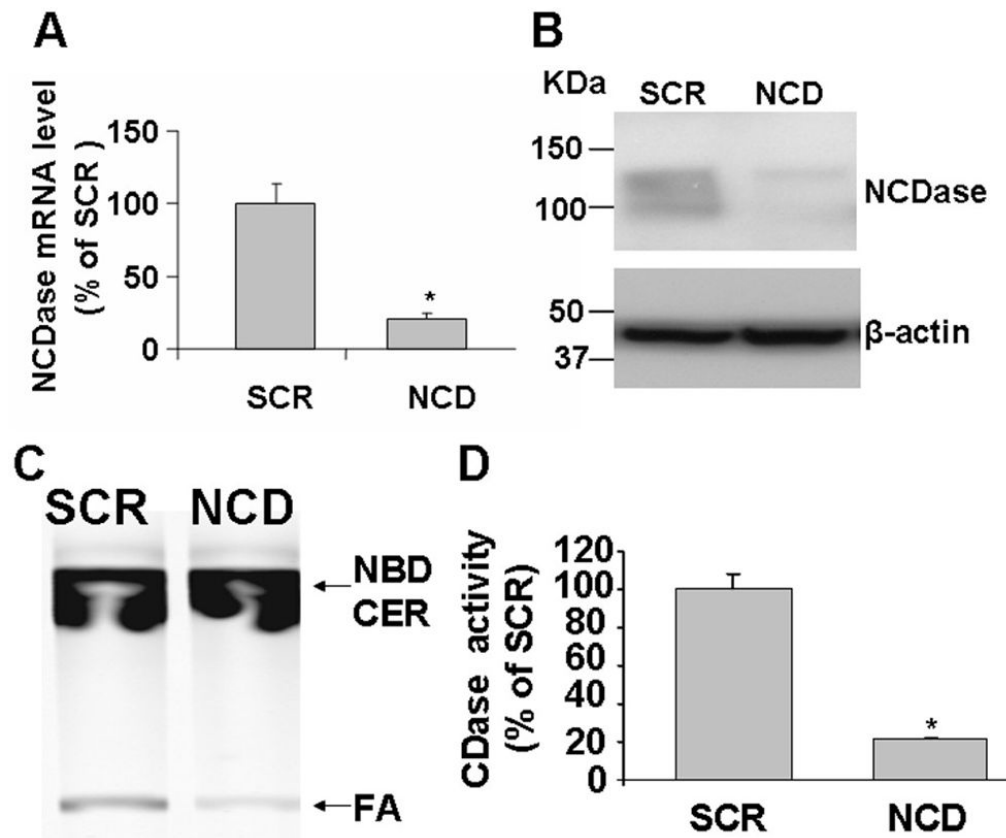


Figure 5. Effectiveness and specificity of NCDase siRNA

Cells were transfected with scrambled siRNA or NCDase siRNA for about 36 hours and then cells were collected, lysed and then subjected to RT-PCR, Western and NCDase activities assays as described under “Materials and Methods”. (A) Real time RT-PCR analysis of NCDase mRNA level. (B) Western blot analysis of endogenous NCDase expression in H. end. cells. Equal loading was verified by using anti- β -actin. (C) TLC analysis of NCDase activity in NCDase siRNA treated cells. (D) NCDase activity was quantified by densitometry. The values are expressed as the mean \pm SD (n=3). Results are representative of three independent experiments. SCR, scrambled siRNA; NCD, NCD siRNAi; FA, fatty acid product; NBD CER, NBD C-12 ceramide substrate. Statistical significance was calculated with respect to scrambled control (*, $p < 0.05$)

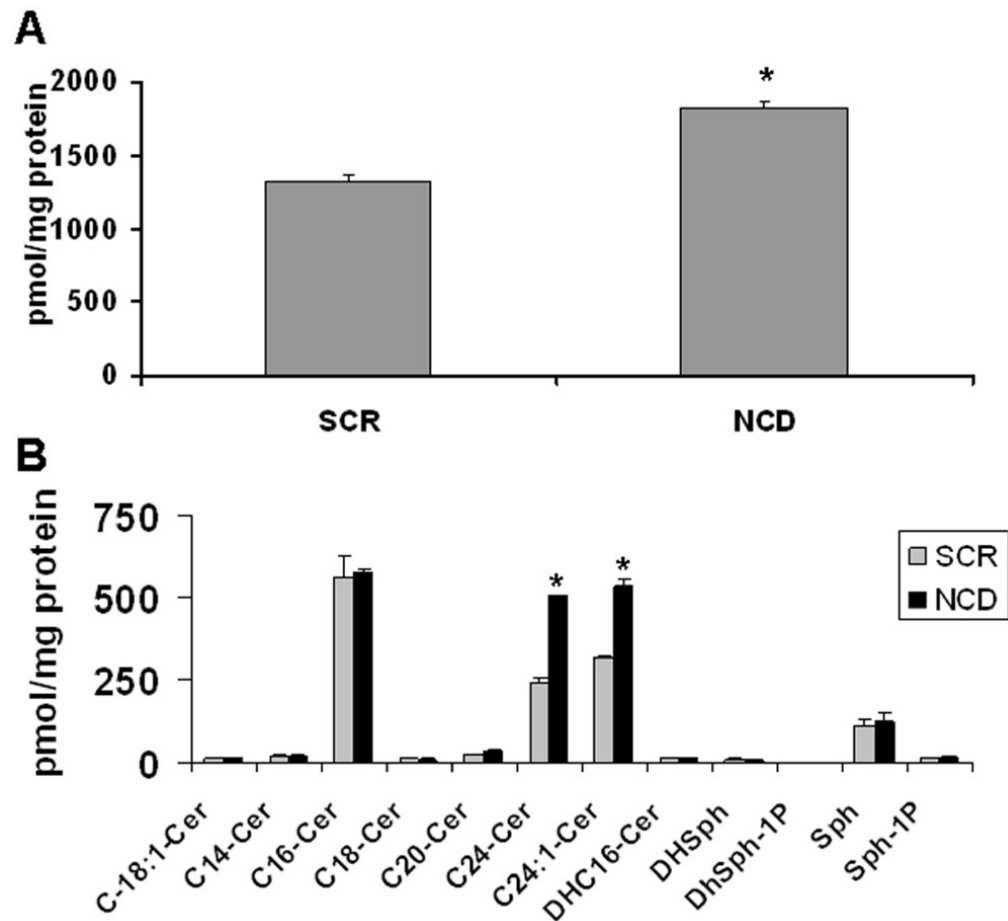


Figure 6. Modulation of ceramide levels by knockdown of NCDase using siRNA in H. end. cells 36 hours after cells were transfected by siRNAs, the changes in ceramide species were analyzed in SCR control and NCDase knockdown cells as described under “Materials and Methods”. (A) Total ceramide. (B) Ceramide-sphingosine profiles. Each sample was normalized to its respective total protein levels. The values are expressed as the mean \pm SD (n=3). Statistical significance was calculated with respect to scrambled control (*, $p < 0.05$).

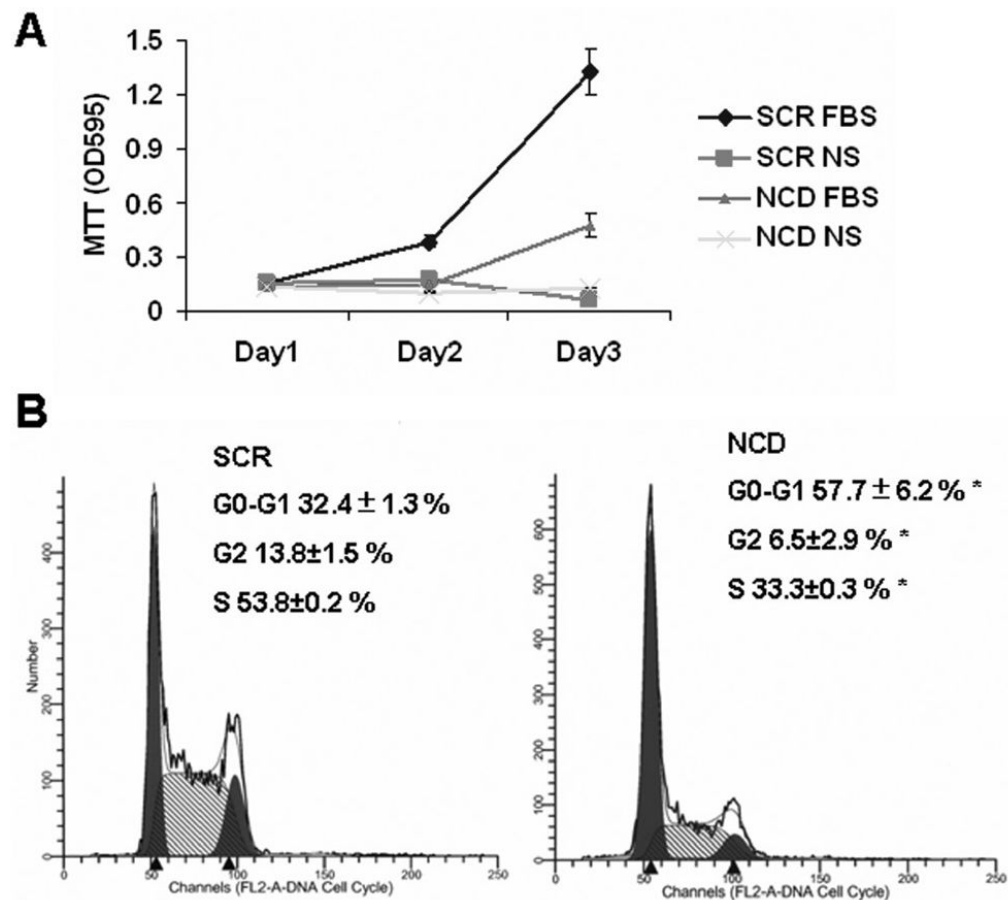


Figure 7. Effects of NCDase siRNA on *H. end.* cell growth and apoptosis

(A) The effects of loss of NCDase on cell growth were determined by MTT assays. 24 hour after transfection using SCR or NCDase siRNAs, cells were split and plated in 6-well plates, the culture media containing either 10% FBS or no serum (NS). Then MTT assays were performed at 0 (day 1 post-transfection), 24, 48 hours after the seeding. (B) The effects of NCDase siRNA on cell cycle profiles were determined and compared with those of nonspecific siRNA-treated cells after 36 h by flow cytometry as described under “Materials and Methods”. The values are expressed as the mean \pm SD (n=3). The results are representative of at least three independent experiments. Statistical significance was calculated with respect to scrambled control (*, $p < 0.05$).

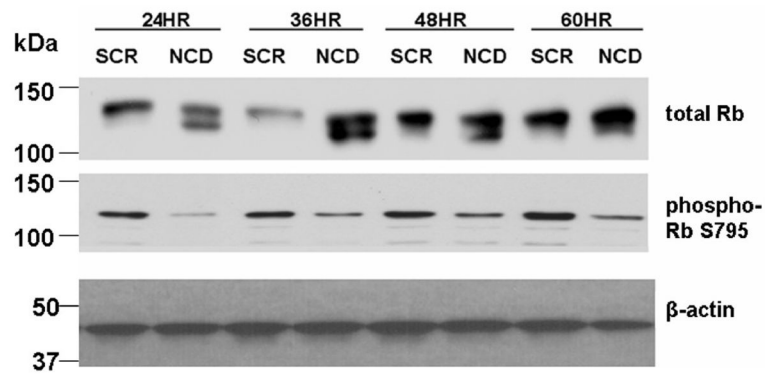


Figure 8. Effects of NCDase siRNA on the state of Rb phosphorylation in H. end. cells
Cells treated with SCR or NCDase siRNA were collected at 24 to 60 hours post treatment. Cell lysates were separated by SDS-PAGE. Total Rb and levels of Phospho-S795-Rb were analyzed by Western blot. Equal loading was verified by using anti- β -actin. The results are representative of at least three independent experiments.